Cardiovascular Diabetology

RESEARCH

Open Access

PACS2/CPT1A/DHODH signaling promotes cardiomyocyte ferroptosis in diabetic cardiomyopathy

Hong Xiang[1,2], Qi Lyu[1], Shuhua Chen[3], Jie Ouyang[4], Di Xiao[1], Quanjun Liu[4], HaiJiao Long[4], Xinru Zheng[4], Xiaoping Yang[1*] and Hongwei Lu[2,4*]

Abstract

Objectives The pathophysiology of diabetic cardiomyopathy (DCM) is a phenomenon of great interest, but its clinical problems have not yet been effectively addressed. Recently, the mechanism of ferroptosis in the pathophysiology of various diseases, including DCM, has attracted widespread attention. Here, we explored the role of PACS2 in ferroptosis in DCM through its downregulation of PACS2 expression.

Methods and results Cardiomyocytes were treated with high glucose and palmitic acid (HGPA), and the detection of cardiomyocyte iron ions, lipid peroxides, and reactive oxygen species (ROS) revealed clear ferroptosis during these treatments. Silencing PACS2 downregulated CPT1A expression and upregulated DHODH expression significantly, reversing HGPA-induced ferroptosis. Further silencing of PACS2 with a CPT1A agonist exacerbated cardiomyocyte ferroptosis while promoting mitochondrial damage in cardiomyocytes. Using a mouse model of type 2 diabetes induced by streptozotocin (STZ) and a high-fat diet (HFD), we found that PACS2 deletion reversed these treatment-induced increases in cellular iron ions, impaired cardiac function, mitochondrial damage and ferroptosis in cardiac muscle tissues.

Conclusions The PACS2/CPT1A/DHODH signalling pathway may be involved in ferroptosis in DCM by regulating cardiomyocyte mitochondrial function.

Keywords Diabetic cardiomyopathy, Ferroptosis, Mitochondria

Introduction

The worldwide prevalence of diabetes is 9.3% (463 million individuals), a figure that is predicted to increase to 10.9% (700 million) by 2045 [1]. Diabetic cardiomyopathy (DCM), which was identified nearly half a century ago [2], is the primary cause of heart failure among diabetic patients [3, 4]. Despite the exponential increase in the number of preclinical and clinical studies on DCM in recent decades, the pathogenesis of this condition has not been fully elucidated.

Hyperglycaemia and hyperlipidaemia represent crucial hallmarks of diabetes and are also pivotal pathogenic

*Correspondence:
Xiaoping Yang
Xiaoping.Yang@hunnu.edu.cn
Hongwei Lu
hongweilu@csu.edu.cn
[1]Key Laboratory of Study and Discovery of Small Targeted Molecules of Hunan Province, Department of Pharmacy, School of Medicine, Hunan Normal University, Changsha, Hunan, China
[2]Center for Experimental Medicine, The Third Xiangya Hospital of Central South University, Changsha, China
[3]Department of Biochemistry, School of Life Sciences of Central South University, Changsha, Hunan, China
[4]Department of Cardiology, Third Xiangya Hospital of Central South University, Changsha, Hunan, China

determinants of the disease. Dyslipidaemia has emerged as the primary instigator in type 2 diabetes progression, suggesting that diabetes is "diabetes mellitus with lipid disorders" [5, 6]. Despite intensive glycaemic control therapy, large-scale population-based clinical inquiries have revealed negligible alterations in the ultimate incidence and resolution of diabetic complications [7, 8]. In the practical context of diabetic complications, sugar and lipids, which are ubiquitously produced, may exert a more deleterious effect on various tissues and organs [9–11]. Consequently, glucolipotoxicity aptly embodies the chronic interplay of hyperglycaemia and hyperlipidaemia in the diabetic milieu, culminating in vascular and tissue injury, including diabetic cardiomyopathy [12, 13]. With the advent of diabetes, heightened systemic glucose levels incite metabolic perturbations, prompting a shift in cardiomyocyte metabolism towards fatty acid utilization and fostering intracellular lipid accrual and subsequent lipotoxicity [14, 15]. Intracellular lipid accumulation can lead to excess reactive oxygen species (ROS), causing cell death and thus diabetic complications [16–18]. Several studies have reported that ROS are strongly associated with ferroptosis [19, 20].

Ferroptosis is a nonapoptotic form of regulated cell death that is induced by overproduction of phospholipid hydroperoxides in an iron-dependent manner. It is morphologically, biochemically, and genetically distinct from apoptosis and necroptosis [21, 22]. Ferroptosis has been implicated in the pathological processes associated with cardiac ischaemia/reperfusion injury and doxorubicin-induced cardiomyopathy [23, 24]. Studies have also reported that ferroptosis plays a role in diabetic cardiomyopathy, but the mechanism is not well understood. Increasing evidence suggests that iron overload in individuals with diabetes increases the risk of insulin resistance and diabetes progression and also aggravates cardiovascular complications via the Fenton reaction [25–27]. Simultaneous increases in ROS and lipid peroxidation exacerbate cellular ferroptosis [28]. Therefore, we aimed to define the role of ferroptosis in DCM pathogenesis.

Phosphofuranic acidic cluster sorting protein 2 (PACS2) is a key protein that regulates metabolic diseases and is expressed in tissues such as the heart, skeletal muscle and brain. PACS2 is involved in membrane trafficking and also mediates cellular mitochondrial function [29, 30]. We previously showed that, under hyperglycaemic and hyperlipidaemic conditions, HGHF induces an increase in PACS2 expression in endothelial cells, causing fatty acid β-oxidation (FAO) alterations in endothelial cells [29], thereby promoting the development of diabetes. However, it is unclear whether PACS2 is involved in the development of DCM. It has been reported in the literature that PACS2 plays a key role in diabetic mice and that the expression of PACS2 is significantly increased in hepatocytes of high-fat-fed ob/ob mice [31]. We found that PACS2 is associated with DCM, but the specific mechanism by which PACS2 regulates DCM remains unclear.

Carnitine palmitoyltransferase 1A (CPT1A) is the rate-limiting enzyme in fatty acid β-oxidation; it catalyses the transfer of long-chain acyl groups from acyl coenzyme A ester to carnitine, allowing fatty acids to enter the mitochondrial matrix for oxidation, and whose deficiency or aberrant regulation leads to metabolic disorders [32]. Fatty acid accumulation promotes the development of insulin resistance, ultimately leading to type 2 diabetes and hyperinsulinaemia [33]. CPT1A has been reported to have significant effects on metabolic syndrome, cardiovascular disease, type 2 diabetes and other diseases [34]. For example, a clinical study of the CPT1A inhibitor etomoxir showed improvement in the course of heart failure but was terminated prematurely due to elevated liver transaminase in enrolled patients [35], which suggest a deleterious effect of CPT1A. However, increasing CPT1A expression can improve lipid metabolic abnormalities such as metabolic syndrome, obesity and type 2 diabetes, and hypertriglyceridemia [36]. Increased CPT1A expression has been shown to significantly reduce hepatic triglyceride levels, and inhibit the JNK factor to prevent the inflammatory response caused by free fatty acids [33]. In addition, insufficient hepatic CPT1A expression leads to steatosis, and liver CPT1A gene therapy reduces diet-induced hepatic steatosis and obesity in mice [37]. These suggest a protective role for CPT1A. The role of CPT1A varies across tissues and pathologies.

Dihydroorotic acid dehydrogenase (DHODH) is a newly identified key protein with anti-ferroptosis properties that scavenges intracellular ROS in human cells and thus inhibits cellular ferroptosis [38]. DHODH activity has been reported to be significantly reduced in tumour cells [38].

In this study, we explored whether PACS2 regulates ferroptosis in cardiomyocytes trefereugh CPT1A/DHODH signalling. We also established a streptozotocin (STZ) and high-fat diet (HFD)-induced type 2 diabetic mouse model [39, 40] to assess the impairment of myocardial ferroptosis. In addition, we used an in vitro model of cardiomyocyte injury [41, 42] induced by HGPA to study the major molecular mechanisms underlying changes in ferroptosis and impairment of mitochondrial function.

Materials and methods

Animal model and study design

All animal manipulations were approved by the Institutional Animal Care and Ethics Committee of Central South University (Approval No.CSU-2023-0158). Eight-week-old male C57BL/6 J wild-type (WT) and

phosphofuranic acid cluster sorting protein 2 (PACS2) knockout ($PACS2^{-/-}$) mice were purchased from Nanjing Institute of Biomedical Research, Nanjing University, and were housed in standard pathogen-free conditions at Xiangya School of Medicine, Central South University, where they were provided with a standardized laboratory diet, with free access to food and water, and with indoor temperature (22 ± 1) and humidity (65–70%) with a 12-h light–dark cycle. At the end of the study, all animals were anesthetized by inhalation of isoflurane (1.5–2%) and then euthanized by bloodletting.

After 1 week of acclimatization, the mice were randomly divided into WT, $PACS2^{-/-}$, HFD, and HFD + $PACS2^{-/-}$ groups of 6 mice each, with the WT and $PACS2^{-/-}$ groups fed a standard diet and the HFD and HFD + $PACS2^{-/-}$ groups fed a HFD (D12109C, Research Diets, New Brunswick, NJ, USA); the latter two HFD groups were given 5 consecutive intraperitoneal injections of 35 mg/kg STZ (S0130, Sigma–Aldrich, San Louis, MO, USA) between 9 and 10 weeks. STZ was dissolved in sodium citrate-hydrochloric acid buffer (SSC) at pH 4.5. The WT and $PACS2^{-/-}$ groups were injected with the same volume of SSC. Blood glucose was measured at 14 weeks, and mice with blood glucose > 11.1 mM were considered diabetic.

Cell culture

H9c2 (CRL-1446) cardiomyocytes were obtained from the American Type Culture Collection, cultured in medium containing glucose 4.5 mM (C11965500BT, DMEM, Gibco, Germany) supplemented with 10% foetal bovine serum (0500, FBS, ScienCell, USA), incubated in a carbon dioxide incubator, and treated with 30 mM glucose and 0.1 mM palmitic acid (PA) (P0500, Sigma–Aldrich, USA) dissolved in 0.5% bovine serum albumin (BSA) for 48 h to simulate HGPA treatment.

Lentiviral transfection of PACS2 shRNA

To construct the rat PACS2-silenced lentivirus (GeneChem production), the hU6-MCS-CMV-puromycin vector was used, and the silencing target sequence was as follows:

sh1: GCGCTACTGCGCAGGTTTAAA;
sh2: AGGCAACAAGCTACAGATCAT;
sh3: AAGCACCAACAGAACATGCTT.

The control lentivirus was inserted with a nonsense sequence: TTCTCCGAACGTGTCACGT. LV-PACS2 was transfected into H9c2 cells (MOI of 20), and PACS2-silenced cells (referred to as shPACS2) and control cells (referred to as Ctrl) were harvested after screening at a final concentration of 4 μg/ml puromycin for 5–7 days. shPACS2 (sh2)- and shPACS2 (sh3)-silenced H9c2 cells accounted for > 90% of the transfected H9c2 cells.

Masson staining

Paraffin sections were deparaffinized sequentially until they were rinsed under running water, and the sections were immersed in Masson A liquid overnight and rinsed under running tap water. The sections were immersed in equal proportions of Masson B and Masson C, stained for 1 min, washed with tap water, differentiated for a few seconds, and washed with tap water. The sections were dipped into Masson D for 6 min, rinsed with tap water, and dyed with Masson E for 1 min. The sections were directly dyed with Masson F for 2–30 s. The sections were rinsed and differentiated with 1% acetic acid and dehydrated in two vats of anhydrous ethanol. The sections were placed in anhydrous ethanol for 5 min, in xylene for 5 min to clear, and with neutral gum to seal the slices.

Label-free quantitative proteomics

After treatment with HGPA for 48 h, the H9c2 cells were collected to extract total protein, and the peptide samples (2 μg) were separated and analysed by Kangchen Biotech Co. Ltd. (Shanghai, China) via the EASY-nLC1200 system and a Q Exactive mass spectrometer (120 min/sample). Differentially expressed peptides with $p < 0.05$ and a fold change > 2 were analysed by Gene Ontology (GO) enrichment via Blast2GO 4.0.7 software.

Western blot analysis

The cells were collected, and total proteins were extracted and subjected to Western blotting with the following antibodies: anti-CPT1A (12252S, Cell Signaling Technology, USA), PACS2 (19508-1-AP, Proteintech, China), GAPDH (60004-1, Proteintech, China), DHODH (ab174288, Abcam, UK), DRP1 (ab184247, Abcam, UK), Mfn2 (ab124773, Abcam, UK) and an HRP-conjugated goat anti-rabbit IgG secondary antibody (PR30011, Proteintech, China).

Haematoxylin and eosin (H&E) staining

To determine whether diabetes alters heart morphology, hearts were collected at the end of the study. The hearts were photographed and fixed with 4% paraformaldehyde. The tissues were then dehydrated, embedded in paraffin blocks, cut into 5-μm-thick sections, and mounted on slides coated with 3-aminopropyltriethoxysilane. The sections were deparaffinized, rehydrated, rinsed in H_2O and stained with haematoxylin–eosin.

Echocardiography

Two-dimensional directional M-mode echocardiographic images were acquired in long-axis and short-axis views at the level of the papillary muscles and recorded at a speed of 66 mm/s. The left ventricular internal diameter and wall thickness were obtained from cross-sectional

short-axis views. The heart rate was recorded simultaneously. The left ventricular shortening rate (LVFS%), ejection fraction (LVEF%), and left ventricular wall thickness were calculated from M-mode tracings. Measurements of diastolic dysfunction, such as the mitral E/e' ratio, were performed from diastolic two-dimensional parasternal short-axis views.

Transmission electron microscopy

After myocardial perfusion, the animals were euthanized and examined via transmission electron microscopy (TEM; Hitachi, Tokyo, Japan). Myocardial tissues were fixed in phosphate buffer solution (PBS) containing 1.25% glutaraldehyde and 2% paraformaldehyde and then postfixed in phosphate buffer solution (PB) containing 1% OsO_4 for 2 h. Tissue blocks smaller than 1 mm^3 were dehydrated, embedded in resin blocks, cut into ultrathin sections of 60–80 nm (Leica, Wetzlar, Germany) and stained with 2% uranyl acetate. Images were captured via TEM.

Assessment of reactive oxygen species

Intracellular ROS production was determined according to the 2′,7′-dichlorodihydrofluorescein diacetate (DCFH-DA) assay provided by the manufacturer (S0033S, Beo Tianmei Biotechnology Institute, Shanghai, China). The cells were washed three times with serum-free ECM, inoculated into 6-well plates at a density of 2×10^5 cells/well, and then incubated with 10 μM DCFH-DA for 30 min at 37 °C. The cells were incubated with 10 μM DCFH-DA for 1 min at 37 °C for 2 min. Subsequently, the cells were washed again and observed under an inverted fluorescence microscope (Olympus Corporation, Tokyo, Japan). The average fluorescence intensity was determined via ImageJ software.

FerroOrange staining

The Fe^{2+} levels in different groups of cardiomyocytes and myocardial tissues were determined via FerroOrange (F374, Dojindo, Japan). The samples were gently rinsed twice with PBS to remove extracellular Fe^{2+}, and a 1 mM FerroOrange stock solution was then diluted with PBS to prepare a staining solution with a final concentration of 1 μM. The staining solution was added to cover the sample. The samples were then incubated in a wet box at 37 °C for 30 min, and the nuclei were labelled with DAPI for 5 min. After staining, the cells were washed twice with PBS for 5 min each and then visualized with a confocal microscope (LSM800, Zeiss, Germany).

Liperfluo staining

Lipid peroxide levels in H9c2 cardiomyocytes and mouse myocardial tissues were measured with Liperfluo (L248, Dojindo, Japan). The samples were gently rinsed twice with PBS, and a staining solution with a final concentration of 5 μM was then prepared by diluting 1 mM Liperfluo stock solution with PBS. The staining solution was added to cover the sample. The samples were then incubated in a wet box at 37 °C for 30 min, and the nuclei were labelled with DAPI for 5 min. After staining, the cells were washed twice with PBS for 5 min each and then visualized with a confocal microscope.

Immunofluorescence staining

The cells were fixed with 4% paraformaldehyde for 15 min, permeabilized with 0.5% Triton X-100 in phosphate buffer solution (PBS) for 10 min and blocked with 1% BSA in PBS for 30 min. The cells were then incubated continuously overnight at 4 °C with primary antibodies against Drp1 (ab184247, Abcam, UK) and Mfn2 (ab12477, Abcam, UK), and the secondary antibody was goat anti-rabbit IgG H&L (Alexa Fluor®488) (ab150077, Abcam, UK) for 1 h at room temperature. The cell nuclei were stained with DAPI (BS097, Biosharp, China) for 5 min at room temperature. The cells were observed via confocal microscopy and digitized via ImageJ software.

Statistical analysis

Statistical analysis was performed via SPSS statistics version 23.0 (IBM, Armonk, New York, USA). All the data are expressed as the means±standard deviations. Comparisons of data between two groups were performed via Student's t test. For data from more than two groups, one-way analysis of variance (one-way ANOVA) was used. $P<0.05$ was considered statistically significant.

Results

HGPA induces ferroptosis and increases PACS2 expression in cardiomyocytes

To explore whether HGPA is associated with ferroptosis in diabetic cardiomyocytes, we treated cardiomyocytes with HGPA for 48 h. The results revealed that ferroptosis was significantly elevated in cardiomyocytes and that the lipid peroxide and ROS contents were increased (Fig. 1A–F). Electron microscopy examination of the mitochondria in both groups of cardiomyocytes revealed that the mitochondria in the HGPA group underwent coupling and thickening of the plasma membrane, and significant ferroptosis occurred (Fig. 1G). Interestingly, protein blotting revealed that PACS2 was highly expressed in the HGPA group compared with the control group, suggesting that PACS2 plays an important role in the development of DCM (Fig. 1H, I). Furthermore, ferroptosis-specific inhibitor ferrostatin-1 (Fer-1) attenuated HGPA-induced levels of the ferroptosis marker ferric ion with lipid peroxidation (see Supplementary material Fig. S1). Collectively, these results suggest that HGPA induced iron death in cardiomyocytes.

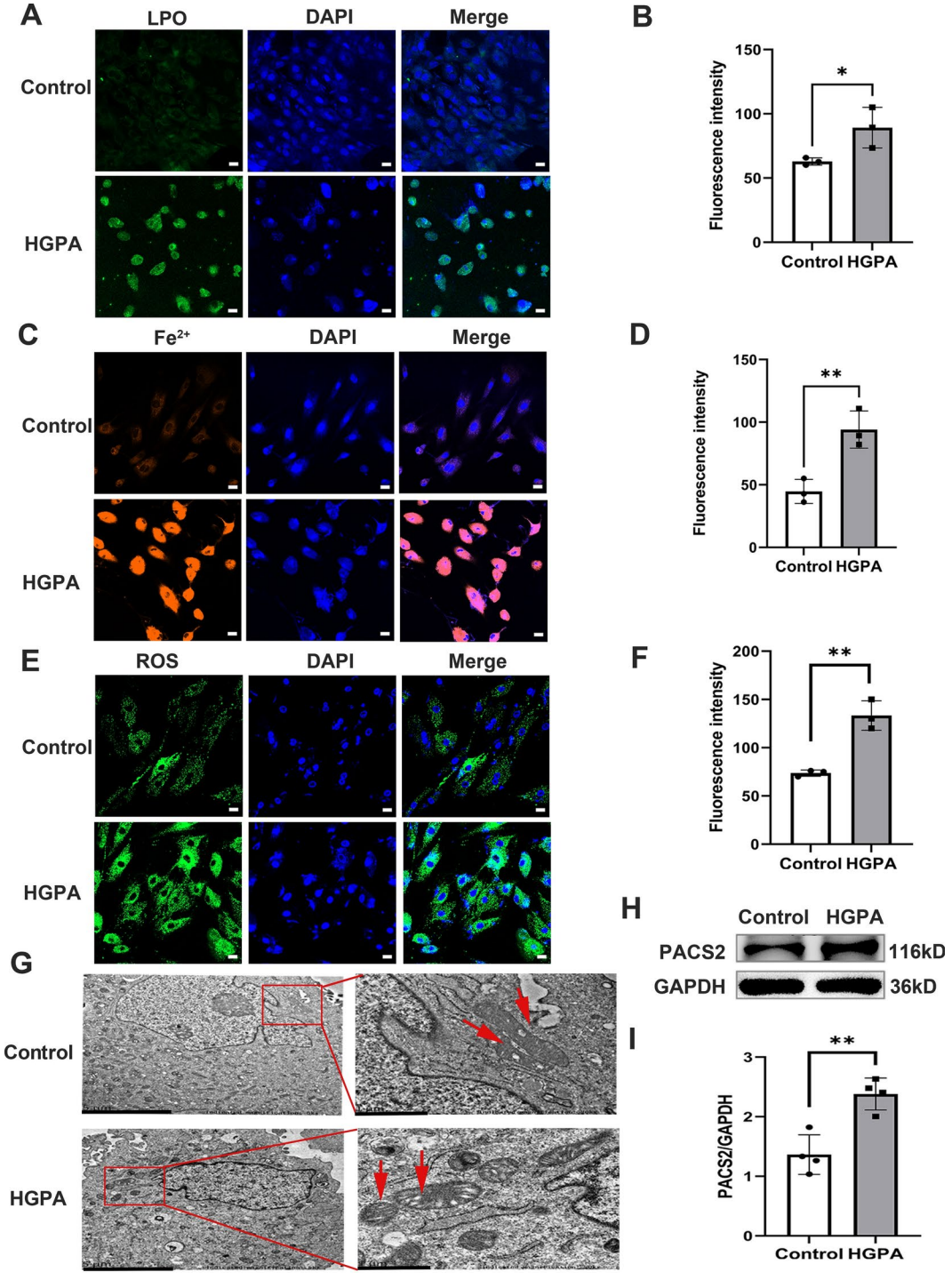

Fig. 1 HGPA significantly increases cardiomyocyte ferroptosis and PACS2 expression. **A**, **B** Comparison of lipid peroxidation fluorescent probe staining results for H9c2 cells in the control and HGPA groups (n = 3). Scale bar = 20 μm. **C**, **D** Fluorescent probe staining for iron ions in H9c2 cells in the control and HGPA groups (n = 3). Scale bar = 20 μm. **E**, **F** Fluorescent probe staining for ROS in H9c2 cells in the control and HGPA groups (n = 3). Scale bar = 20 μm. **G** Mitochondrial changes in H9c2 cells detected by transmission electron microscopy after HGPA treatment. Scale bar = 5 μm. Scale bar = 1 μm. **H** PACS2 protein expression in HGPA-treated H9c2 cells (n = 3). Graphs show mean ± SD. statistical significance was analyzed using Student's t-test and one-way ANOVA. *$p < 0.05$; **$P < 0.01$

PACS2 silencing inhibits cardiomyocyte ferroptosis

To explore the relationship between PACS2 and ferroptosis, PACS2 expression was silenced in cardiomyocytes, and sh2 and sh3, which had better silencing effects, were selected (Fig. 2A, B). Additionally, the contents of iron ions and lipid peroxides in cardiomyocytes were detected, and the results revealed significant reversal of iron ions and lipid peroxides in the HGPA plus PACS2-silenced group compared with those in the HGPA group (Fig. 2C–F). Electron microscopy results showed that mitochondrial plasma membrane thickening was somewhat restored after silencing PACS2 compared with the HGPA group (Fig. 2G). This suggests that silencing PACS2 can reverse the cardiomyocyte ferroptosis.

HGPA leads to cardiomyocyte ferroptosis via PACS2/CPT1A/DHODH signalling

GPX4 and DHODH are the key proteins involved in preventing ferroptosis [43, 44]. To explore the possible pathways of ferroptosis induced by HGPA, cardiomyocytes were treated with HGPA, and protein blotting was performed to detect GPX4 and DHODH levels. Interestingly, there was no significant difference in the expression of GPX4 between the HGPA group and the control group, whereas the expression of DHODH was significantly lower in the HGPA group (Fig. 3A). Proteomic analysis was used to screen proteins with a 1.5-fold difference in size, and KEGG pathway analysis revealed that the proteins were enriched mainly in fatty acid metabolism. On the basis of the size of the difference in fatty acid metabolism, a significant difference in the expression of carnitine palmitoyltransferase (CPT1A) was detected (Fig. 3D, E). As verified by protein blotting, CPT1A was significantly higher in the treatment group than in the control group (Fig. 3F, G).

CPT1A downregulation inhibits cardiomyocyte ferroptosis

To further validate the specific regulatory mechanism of PACS2-mediated ferroptosis in cardiomyocytes, we used protein blotting to examine the expression of PACS2, CPT1A and DHODH and found that the expression of PACS2 and CPT1A was upregulated and that the expression of DHODH was downregulated in the HGPA group compared with the control group. In contrast, the expression of CPT1A and DHODH was reversed by silencing PACS2 (Fig. 4A–D), indicating that HGPA-induced PACS2 activated the fatty acid β-oxidation pathway, which suppressed DHODH (Fig. 4A–D). Next, we activated CPT1A with its agonist C75 on the basis of PACS2 silencing, detected the expression of CPT1A and DHODH via protein blotting, and found that the expression of CPT1A was elevated and that the expression of DHODH was decreased in the agonist group compared with the silencing-only group (Fig. 4E–G). We detected ferric ions, lipid peroxides, and ROS in these groups via fluorescent probes and confirmed that, in the agonist treatment group, the expression of ferric ions, lipid peroxides and ROS was greater than that in the silenced group (Fig. 4E–H). These findings suggest that silencing PACS2 inhibits cardiomyocyte ferroptosis through the downregulation of CPT1A.

Mitochondrial damage induces ferroptosis in cardiomyocytes via the PACS2/CPT1A/DHODH signalling pathway

Mitochondrial dysfunction leads to cardiomyocyte ferroptosis [45]. The state of type 2 diabetes causes altered mitochondrial dynamics—an imbalance between fission and fusion—with increased expression of the fission protein DRP1 and decreased expression of the fusion protein MFN2, leading to mitochondrial dysfunction [46, 47]. To verify whether PACS2 regulates cardiomyocyte ferroptosis through mitochondrial function, we used protein blotting to detect the mitochondrial splitting protein DRP1 and the fusion protein MFN2 and found that the expression of DRP1 in the HGPA group was elevated compared with that in the control group, whereas silencing PACS2 reversed this increase in DRP1 expression. In contrast, MFN2 expression was decreased in the HGPA group, and this decrease was reversed by silencing PACS2 (Fig. 5A–C). Immunofluorescence was also used to detect DRP1 and MFN2 fluorescence intensity, revealing that DRP1 fluorescence intensity was significantly greater in the HGPA group than in the control group and that mitochondrial function was significantly improved after PACS2 was silenced. Meanwhile, the MFN2 fluorescence content was lower in the HGPA group than in the control group, and silencing PACS2 reversed the increase in MFN2 fluorescence content (Fig. 5D–G). On the other hand, after HGPA treatment, we observed that mitochondria in the HGPA group became fragmented and swollen, whereas silencing PACS partially normalized mitochondrial morphology (see Supplementary material Fig. S2A, B). We then assayed mitochondrial function in cardiomyocytes by adding oligomycin, FCCPand rotenone/antimycotic reagents, and showed that silencing PACS2 restored basal, ATP-generating coupling, and maximal oxygen consumption rate (OCR) after HGPA treatment (see Supplementary Material Fig. S2C, D) Next, we interfered H9c2 cells with shPACS2, activated CPT1A with C75 and then treated them with HGPA, and detected the expression of DRP1 and MFN2 by protein blotting, and found that shPACS2 down-regulated the expression of DRP1 and up-regulated the expression of MFN2 compared to HGPA-treated group, whereas the activation of CPT1A reversed the expression of DRP1 and MFN2 (Fig. 5H–J). These data suggest that PACS2

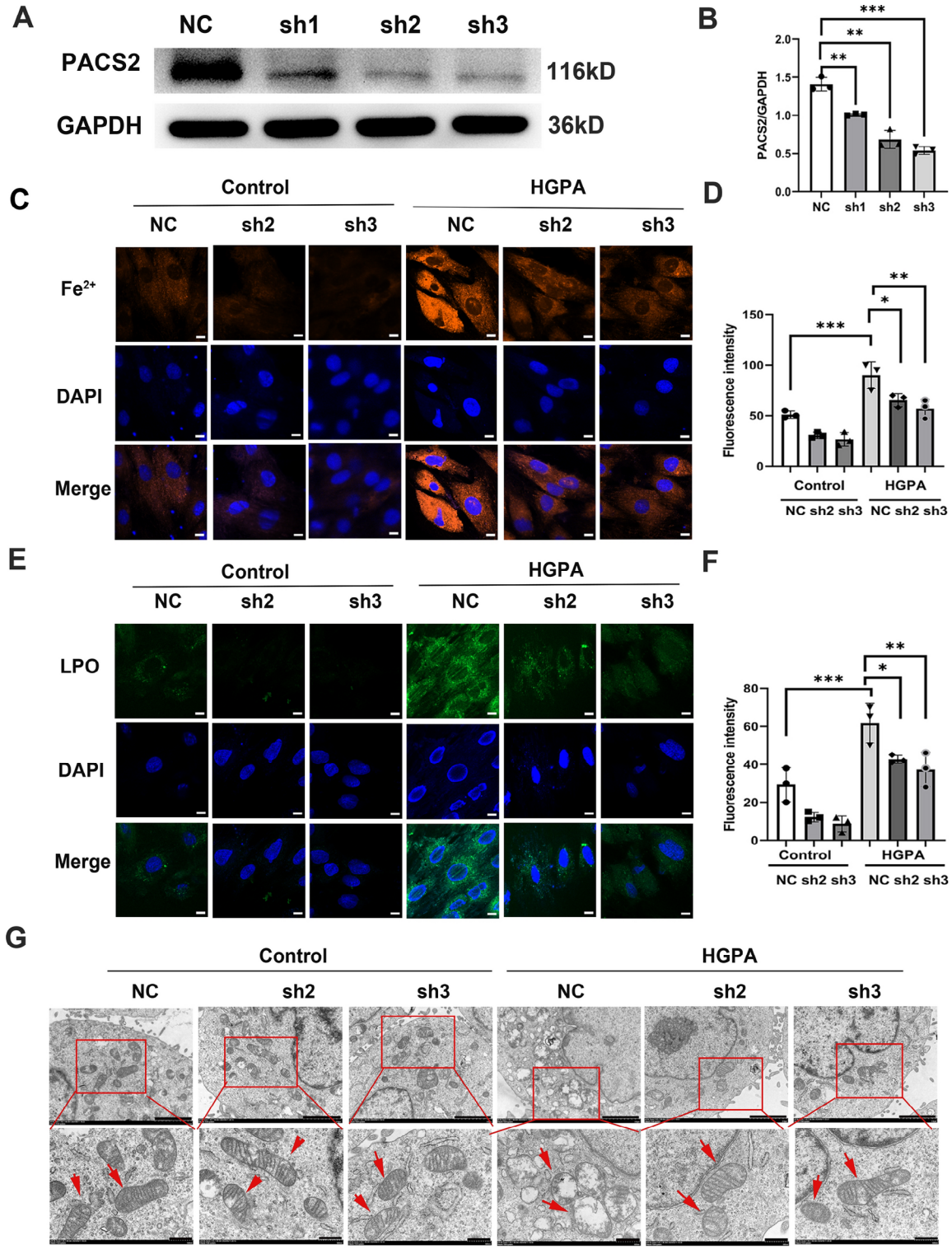

Fig. 2 Silencing PACS2 blocks ferroptosis in cardiomyocytes. **A**, **B** Three PACS2 silencing sequences were selected to infect H9c2 cells, and sh2 and sh3, which have good silencing effects, were selected (n = 3). **C**, **D** Detection of iron ions by a fluorescent probe after PACS2 silencing in the control and HGPA intervention groups of H9c2 cells (n = 3). Scale bar = 20 μm. **E**, **F** When PACS2 was silenced, HGPA intervention in H9c2 cells was followed by the use of a fluorescent probe to detect the lipid peroxide content in each group (n = 3). Scale bar = 20 μm. **G** Mitochondria were detected by transmission electron microscopy after PACS2 silencing and HGPA intervention in H9c2 cells. Scale bar = 20 μm. Graphs show mean ± SD, and one-way ANOVA was used for multiple group comparisons. *$p < 0.05$;**$P < 0.01$; ***$P < 0.001$

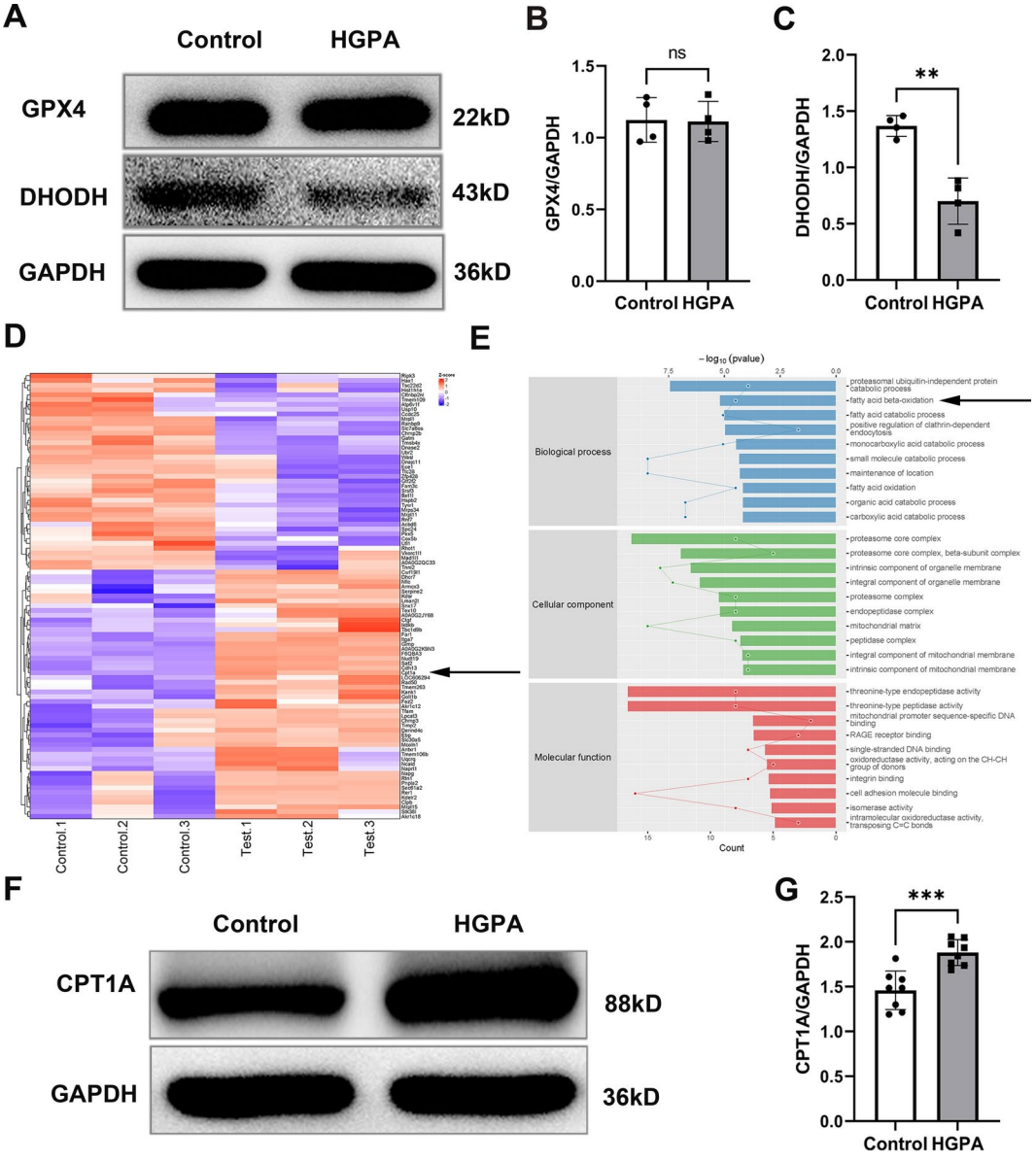

Fig. 3 PACS2 induces cardiomyocyte ferroptosis via CPT1A/DHODH signalling. **A**–**C** GPX4 and DHODH expression was detected by protein blotting in each group after HGPA intervention (n = 3). **D** Proteomic heatmap after HGPA intervention. **E** KEGG enrichment map. **F**, **G** Protein blotting of CPT1A expression after HGPA intervention (n = 6). Graphs show mean ± SD. Statistical significance was determined using Student's t-test for two group's comparison.**$P < 0.01$; ***$P < 0.001$; ns, not significant

regulates mitochondrial function to promote ferroptosis in cardiomyocytes.

Knockdown of PACS2 reverses ferroptosis in mouse myocardial tissue

To explore high-fat diet-induced histopathological changes and ferroptosis in the mouse myocardium, we constructed a diabetic mouse model. High-fat feeding plus low-dose STZ injection for 14 weeks resulted in hyperglycaemia and weight gain (Fig. 6A, B). To verify the differences between the HFD group and the HFD + PACS2$^{-/-}$ group, a diabetic mouse knockout model was constructed (see Supplementary material Figs. S3, S4), in which fasting blood glucose, total cholesterol, and triglyceride levels were significantly elevated in the HFD group compared with those in the WT group, and the levels of all three indices were somewhat reversed in the HFD + PACS2$^{-/-}$ group (Fig. 6C–E). Echocardiographic evaluation revealed that diastolic function (E/e'), left ventricular ejection fraction (LVEF%), and left ventricular short-axis shortening (LVFS%) were lower in the HFD group than in the WT group, suggesting that cardiac dysfunction and the levels of E/e', LVEF%, and LVFS% were reversed in the HFD + PACS2$^{-/-}$ group

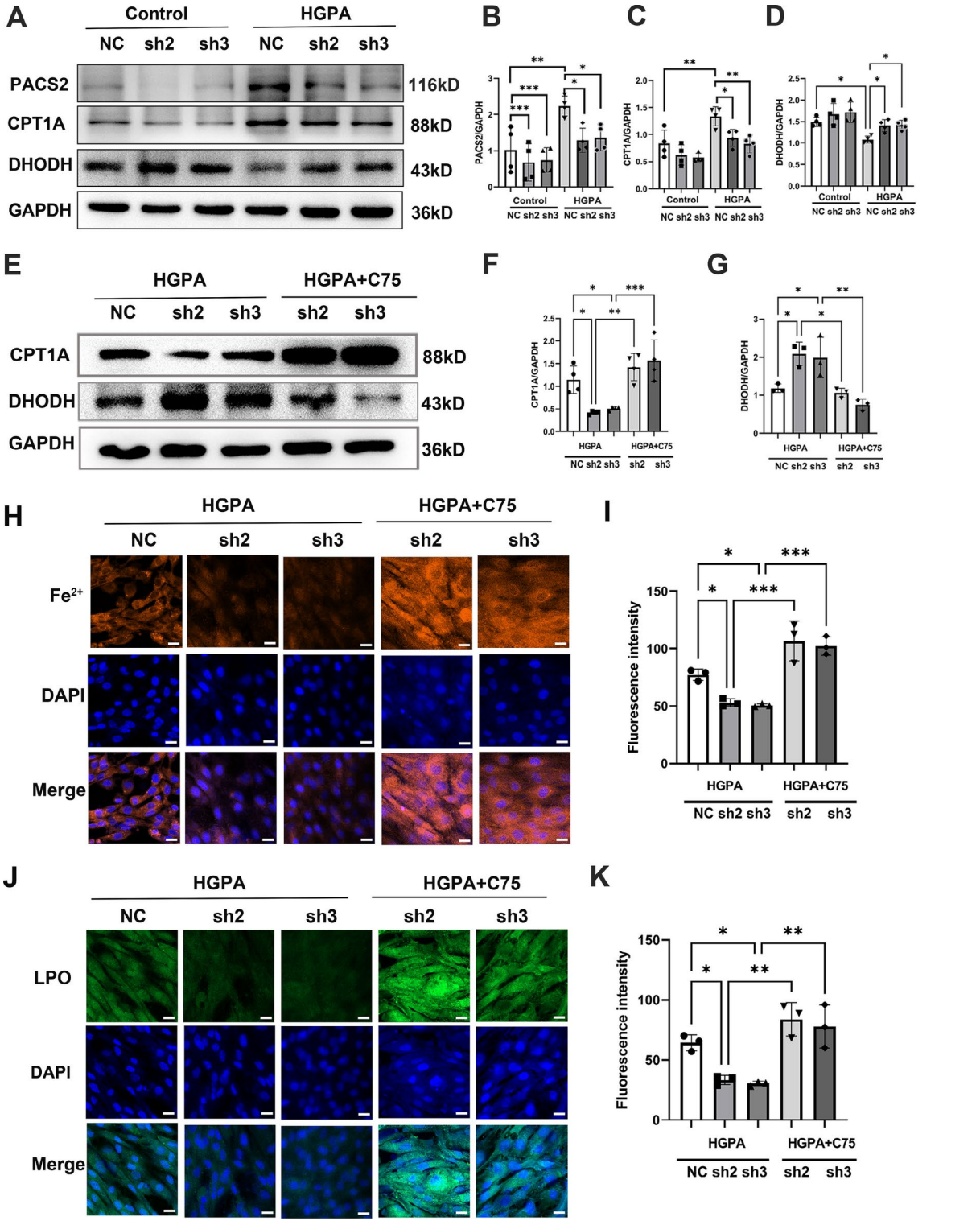

Fig. 4 The inhibition of ferroptosis by PACS2 silencing is dependent on CPT1A reduction in cardiomyocytes. **A**–**D** After HGPA intervention and PACS2 silencing, protein blotting was used to detect the expression of PACS2, CPT1A and DHODH in each group (n = 4). **E**–**G** H9c2 cells were treated with 10uM CPT1A agonist C75 for 24 h, plus HGPA, and protein blotting was performed to detect the expression of CPT1A and DHODH. (n = 4). **H**, **I** C75-treated H9c2 cells were assayed with a fluorescent probe to detect the content of iron ions in each group (n = 3). Scale bar = 20 μm. **J**, **K** C75-treated H9c2 cells with a fluorescent probe to detect the content of lipid peroxides (n = 3). Scale bar = 20 μm. Graphs show mean ± SD, and one-way ANOVA was used for multiple group comparisons. **P* < 0.05;***P* < 0.01; ****P* < 0.001

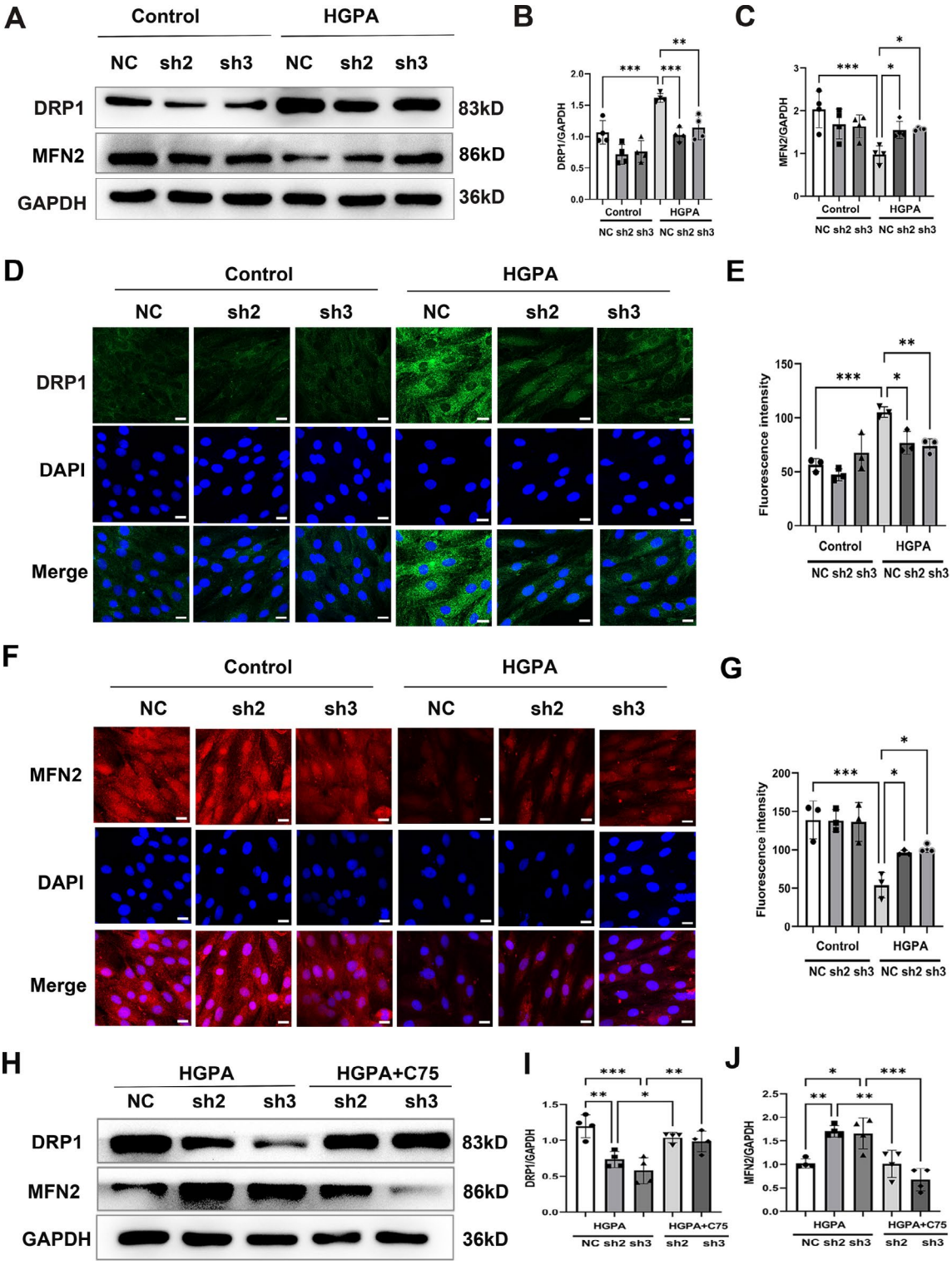

Fig. 5 Silencing PACS2 attenuates the cardiomyocyte ferroptosis induced by impaired mitochondrial function. **A**–**C** after HGPA induction and PACS2 silencing, protein blotting was used to detect the expression of the mitochondrial proteins DRP1 and MFN2 (n = 4). **D**, **E** Silencing of PACS2, HGPA-treated H9c2 cells, and expression of the mitochondrial protein DRP1 was detected by immunofluorescence (n = 3). Scale bar = 20 μm. **F**, **G** Silencing of PACS2, HGPA-treated H9c2 cells, and immunofluorescence to detect the expression of mitochondrial protein MFN2 (n = 3). Scale bar = 20 μm. **H**–**J** PACS2 was silenced, H9C2 cells were treated with C75, then treated with HGPA, and the expression of DRP1 and MFN2 proteins was detected by western blotting. Graphs show mean ± SD, and one-way ANOVA was used for multiple group comparisons. *$P < 0.05$;**$P < 0.01$; ***$P < 0.001$

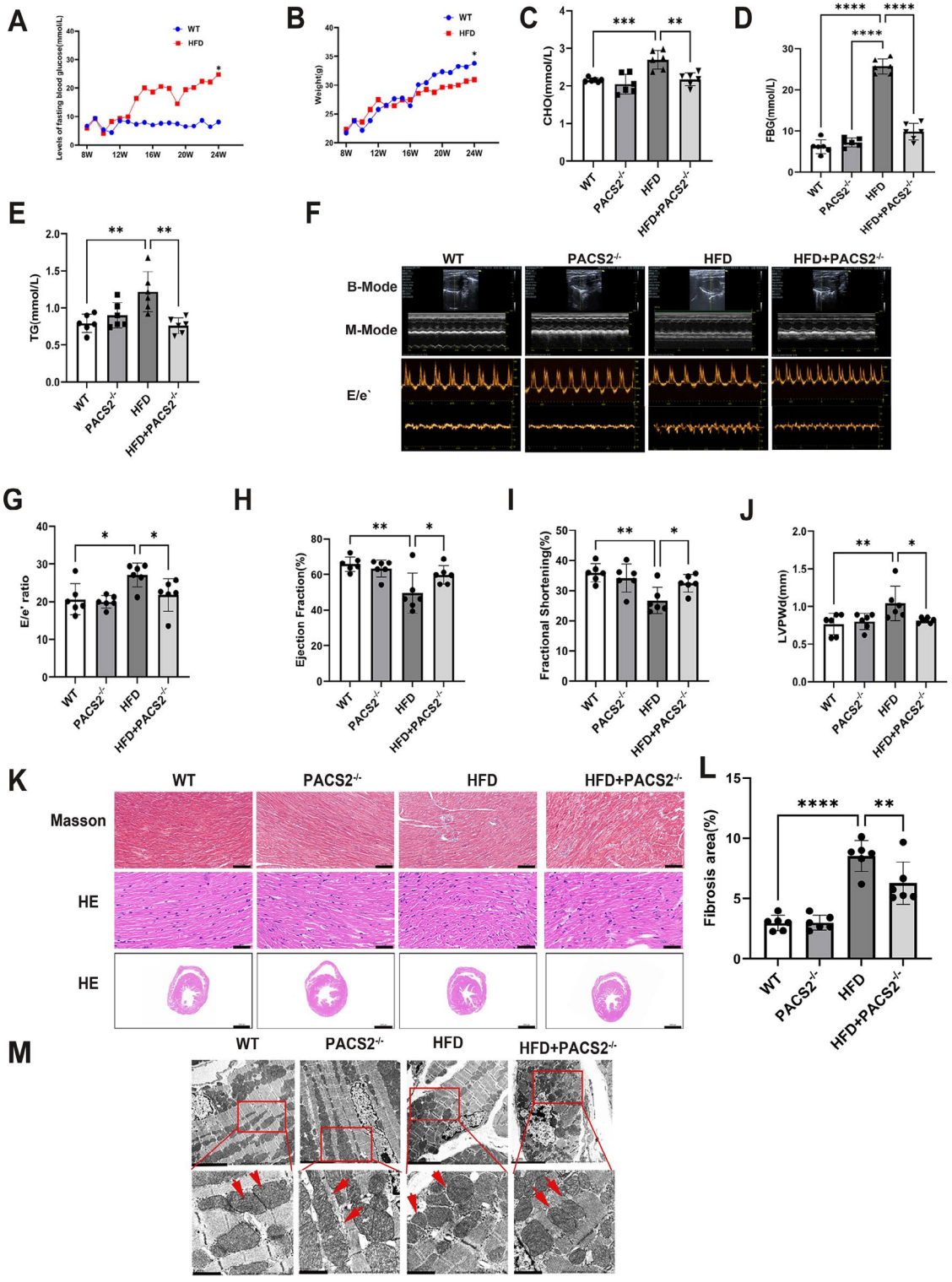

Fig. 6 Ferroptosis is inhibited in the myocardial tissue of PACS2 knockout mice. **A** In the diabetes mouse model, fasting blood glucose was detected at different time points (n = 6). **B** Body weights of the mice at different ages (n = 6). **C**–**E** Peripheral blood triglyceride, fasting blood glucose, and cholesterol levels in the 4 groups of mice (n = 6). **F**–**J** M-ultrasound indices of 4 groups of mice: ejection fraction, short-axis frequency, diastolic function, and left ventricular posterior wall (n = 6). **K**, **L** Morphology of the 4 groups as determined by HE and Masson staining (n = 6). Scale bar = 20 μm. Scale bar = 2000 μm. **M** Mitochondrial alterations in mouse myocardial tissue in the 4 groups were detected by transmission electron microscopy. Scale bar = 5 μm. Scale bar = 1 μm. Graphs show mean ± SD. statistical significance was analyzed using Student's t-test and one-way ANOVA. *$p < 0.05$; **$P < 0.01$; ***$p < 0.001$; ****$p < 0.0001$

(Fig. 6F–J). Morphology revealed that myocardial tissue hypertrophy and fibrosis in HE- and Masson-stained myocardial tissue were reversed in the HFD + PACS2$^{-/-}$ group compared with those in the WT group (Fig. 6K, L). These results suggest that diabetes causes cardiac insufficiency and cardiomyocyte hypertrophy and fibrosis. Furthermore, we examined the changes in the mitochondria of mouse cardiomyocytes via transmission electron microscopy, and the results revealed significant ferroptosis in the mitochondria of mouse cardiomyocytes compared with those of the WT cardiomyocytes, and the ferroptosis phenomenon was reversed in the HFD + PACS2$^{-/-}$ group (Fig. 6M). These results suggest that high-fat diet-fed mice exhibit ferroptosis in myocardial tissue, which is reversed in PACS2 knockout mice.

Mitochondrial injury induces ferroptosis in mouse myocardial tissues via PACS2/CPT1A/DHODH signalling

To validate the regulatory role of the PACS2/CPT1A/DHODH pathway in diabetic cardiomyopathy in vivo, protein blotting was used to detect the protein expression of PACS2, CPT1A and DHODH, and the results revealed that, compared with that in the WT group, the expression of PACS2 and CPT1A was upregulated in the HFD group, the expression of DHODH was downregulated in the HFD group, and the expression of CPT1A and DHODH in the HFD + PACS2$^{-/-}$ group was reversed. Moreover, we verified the expression of the mitochondrial proteins DRP1 and MFN2, the expression of which was elevated in the HFD group compared with the WT group and reversed by the knockdown of PACS2, and the expression of MFN2 was reduced in the HFD group compared with the WT group and reversed by the knockdown of PACS2 (Fig. 7A–F). we used fluorescent probes to detect iron metabolism, lipid peroxidation, and ROS in mouse myocardial tissue. The results showed that the fluorescence amount of ferroptosis, lipid peroxidation and ROS in the HFD group was differently elevated compared with the WT group, and the fluorescence content of the group of HFD + PACS2$^{-/-}$ was reversed (Fig. 7G–J). These findings confirmed that, under high-fat conditions, the PACS2 pathway leads to cardiomyocyte ferroptosis by promoting DCM mitochondrial dysfunction.

Discussion

This study aimed to explore the role of PACS2 in DCM myocardial ferroptosis. We first found that PACS2 was significantly upregulated in the myocardial tissues and cardiomyocytes of DCM mice. By exploring the regulation of PACS2, we found that the PACS2/CPT1A/DHODH signalling pathway is involved in myocardial mitochondrial function and ferroptosis. Thus, it is reasonable to further observe that silencing PACS and agonizing CPT1A reversed HGHF-induced ferroptosis in cardiomyocytes in vitro and reversed high-fat-fed mouse-induced ferroptosis in myocardial tissue in vivo. We also found that the PACS2/CPT1A/DHODH signalling pathway leads to cardiomyocyte ferroptosis by regulating mitochondrial function. Thus, the present study elucidated the possible role and mechanism of the PACS2/CPT1A/DHODH signalling pathway in DCM cardiomyocytes (as shown in the diagram in Fig. 8).

Since PACS2 can regulate a variety of cellular functions, it has been implicated in the development of various diseases, and PACS2 is involved in both membrane transport and metabolism [48]. In 2005, Köttgen et al. suggested that PACS2 is involved in the transport of polycystin-2 [49]. HGPA-induced chronic obesity has been reported to cause DCM [50, 51]. Apparently, PACS2 plays an important role in DCM, although it has not been fully elucidated.

In a high glucose- and high fat diet-induced diabetic cardiomyopathy model, PACS2 affects mitochondrial function by promoting increased ROS production in cardiomyocytes, thereby causing obesity in mice [30]. In vivo experiments also confirmed that silencing PACS2 could reverse the myocardial damage caused by high-fat feeding in mice. Our previous study revealed that PACS2 is closely associated with DCM complications [29]. However, whether PACS2 directly regulates diabetic cardiomyopathy has not been explored. In the present study, we report for the first time that the expression of PACS2 is significantly upregulated in DCM cardiomyocytes and that silencing PACS2 reverses ferroptosis in the myocardium via HGHF. Although ferroptosis is only one mode of cardiomyocyte death, the reversal of cardiomyocyte ferroptosis reduces mitochondrial dysfunction and lipid peroxidation, thereby reducing myocardial injury and ferroptosis.

DHODH is an important regulator of the antioxidant response that can reduce CoQ to CoQH2 in the inner mitochondrial membrane and scavenge lipid peroxides in cells [38]. Studies have shown that the activation of PACS2 generates large amounts of ROS [31], DHODH scavenging is insufficient, and high-glucose and high-fat conditions induce the continuous generation of large amounts of ROS, i.e., an imbalance between the generation and scavenging capacity of ROS, leading to cellular ferroptosis [52]. Previous research has shown that PACS2 activation causes a decrease in fatty acid β-oxidation in DCM endothelial cells, but interestingly, in cardiomyocytes, we found that PACS2 activation causes an increase in fatty acid β-oxidation, which may be related to the need for a large amount of oxidative energy in the mitochondria of cardiomyocytes [53]. CPT1A produces many byproducts in the fatty acid β-oxidation reaction while supplying energy, and DHODH, which scavenges ROS, is inhibited, causing excess ROS in metabolizing

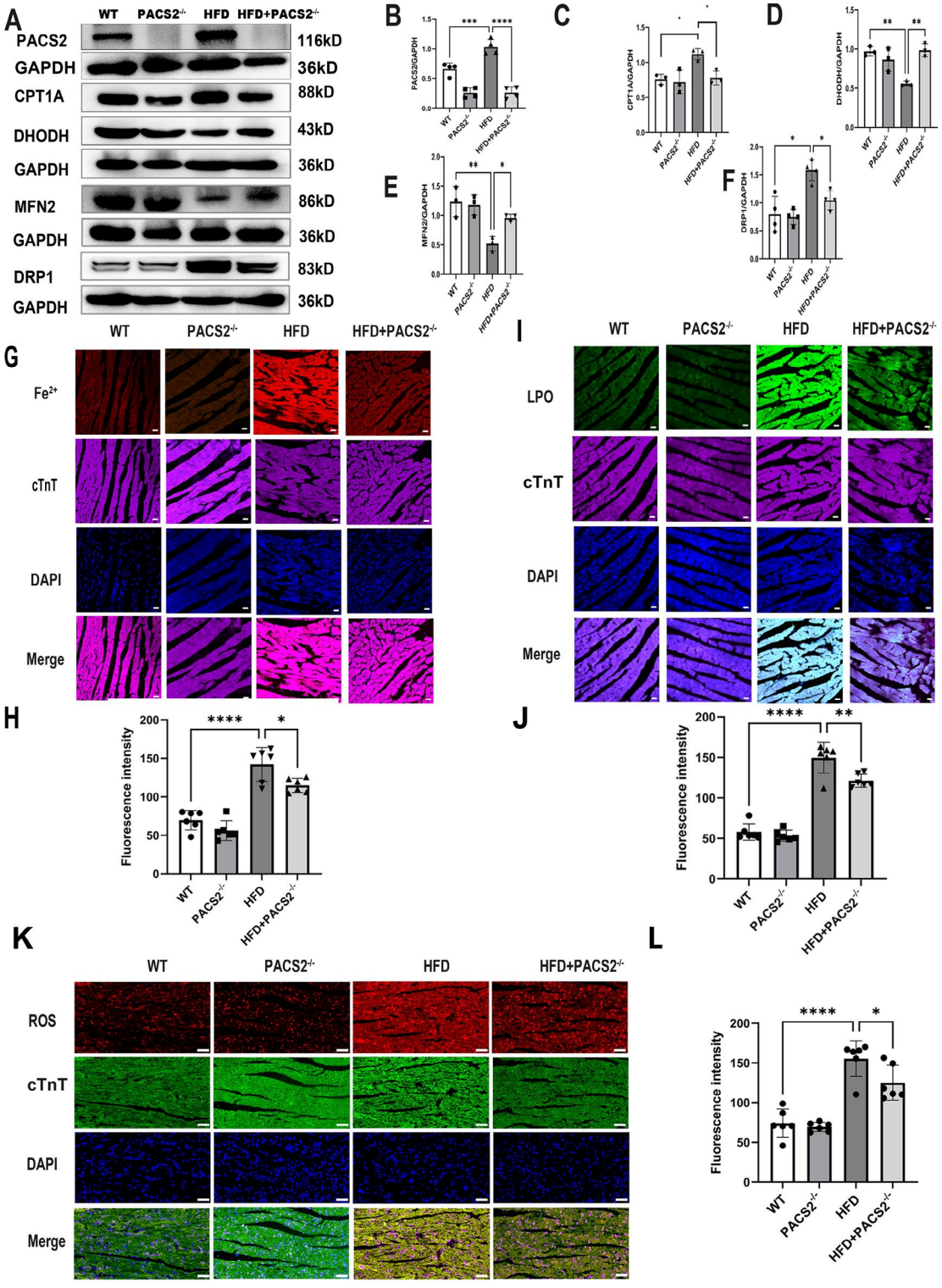

Fig. 7 PACS2 induces ferroptosis in myocardial tissue via CPT1A/DHODH signalling. **A**–**F** Protein blotting was used to detect the expression of PACS2, CPT1A, DHODH and the mitochondrial proteins MFN2 and DRP1 in the myocardial tissues of the 4 groups (n = 3). **G**, **H** Detection of iron ions and Immunofluorescence of Cardiac Troponin T (cTnT) in 4 Groups of Myocardial Tissues Using Fluorescent Probes (n = 6). Scale bar = 20 μm. **I**, **J** Detection of Lipid Peroxides and Immunofluorescence for Cardiac Troponin T (cTnT) in 4 Groups of Myocardial Tissues by Fluorescent Probes (n = 6). Scale bar = 20 μm. **K**, **L** Detection of ROS and Immunofluorescence for Cardiac Troponin T (cTnT) in 4 Groups of Myocardial Tissues by Fluorescent Probes (n = 6). Scale bar = 20 μm. Graphs show mean ± SD, and one-way ANOVA was used for multiple group comparisons. *$P < 0.05$;**$P < 0.01$; ***$P < 0.001$;****$p < 0.0001$

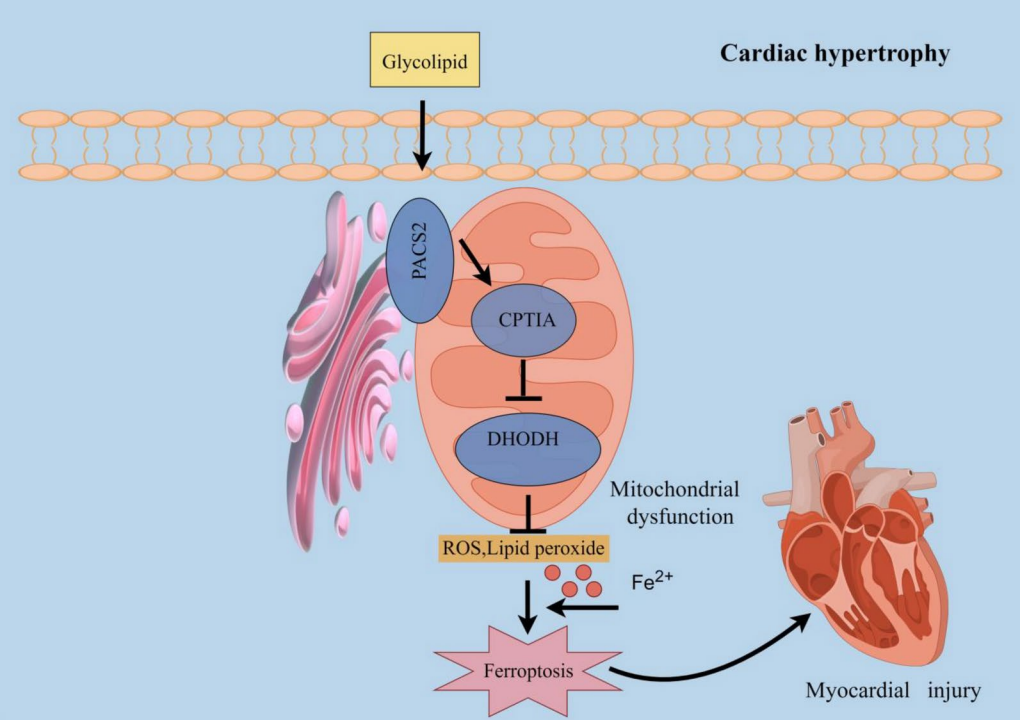

Fig. 8 Diagram of the ferroptosis mechanism via PACS2/CPT1A/DHODH signalling in DCM

cells and ultimately leading to cardiomyocyte ferroptosis. Maintenance of mitochondrial integrity is critical for the myocardial energy supply. However, in diabetic cardiomyopathy, both the mitochondrial fusion and fission processes are dysregulated, with increased fission and decreased fusion [50], as confirmed by our experiments. There, an increase in the fission protein DRP1 as well as a decrease in the fusion protein MFN2 led to mitochondrial dysfunction, attenuated ROS scavenging, and ultimately cardiomyocyte ferroptosis.

In summary, in this study, we found for the first time that PACS2 is elevated in DCM cardiomyocytes. The increased PACS2 and enhanced PACS2/CPT1A/DHODH signalling may concurrently contribute to cardiomyocyte pathogenesis and thus cause cardiomyocyte ferroptosis. Mechanistically, PACS2/CPT1A/DHODH signalling may act by regulating mitochondrial function in cardiomyocytes. Thus, our study suggests that PACS2 could be a novel potential therapeutic target for DCM.

Supplementary Information

The online version contains supplementary material available at https://doi.org/10.1186/s12933-024-02514-6.

Additional file 1.

Acknowledgements
We thank for the Key Laboratory of Study and Discovery of Small Targeted Molecules of Hunan Province, Department of Pharmacy, School of Medicine, Hunan Normal University and the Center for Experimental Medicine, Third Xiangya Hospital, the Central South University, the National Natural Science Foundation of China.

Author contributions
Hong Xiang: Conceptualization, Methodology, Investigation, Data curation, Writing – original draft. Qi Lyu: Formal analysis, Investigation. Shuhua Chen: Formal analysis, Conceptualization. Di Xiao: Supervision, Methodology. Jie Ouyang: Supervision, Visualization. Quanjuan Liu: Supervision, Investigation. Haijiao Long: Investigation. Xinru Zheng: Methodology. Xiaoping Yang and Hongwei Lu: Conceptualization, Funding acquisition, Project administration, Writing – review & editing. All authors reviewed the manuscript.

Funding
This work was supported by the grants from the National Natural Science Foundation of China (Grant No. 82270519, 81870352) and the Natural Science Foundation of Hunan Province (2023JJ30838).

Data availability
No datasets were generated or analysed during the current study.

Declarations

Competing interests
The authors declare no competing interests.

Received: 9 August 2024 / Accepted: 17 November 2024
Published online: 04 December 2024

References

1. Saeedi P, Petersohn I, Salpea P, Malanda B, Karuranga S, Unwin N, Colagiuri S, Guariguata L, Motala AA, Ogurtsova K, et al. Global and regional diabetes prevalence estimates for 2019 and projections for 2030 and 2045: results from the International Diabetes Federation Diabetes Atlas, 9(th) edition. Diabetes Res Clin Pract. 2019;157: 107843.

2. Rubler S, Dlugash J, Yuceoglu YZ, Kumral T, Branwood AW, Grishman A. New type of cardiomyopathy associated with diabetic glomerulosclerosis. Am J Cardiol. 1972;30(6):595–602.
3. Boudina S, Abel ED. Diabetic cardiomyopathy, causes and effects. Rev Endocr Metab Disord. 2010;11(1):31–9.
4. Mizamtsidi M, Paschou SA, Grapsa J, Vryonidou A. Diabetic cardiomyopathy: a clinical entity or a cluster of molecular heart changes? Eur J Clin Invest. 2016;46(11):947–53.
5. Lytrivi M, Castell AL, Poitout V, Cnop M. Recent insights into mechanisms of β-cell Lipo- and glucolipotoxicity in type 2 diabetes. J Mol Biol. 2020;432(5):1514–34.
6. Prentki M, Corkey BE. Are the beta-cell signaling molecules malonyl-CoA and cystolic long-chain acyl-CoA implicated in multiple tissue defects of obesity and NIDDM? Diabetes. 1996;45(3):273–83.
7. Coca SG, Ismail-Beigi F, Haq N, Krumholz HM, Parikh CR. Role of intensive glucose control in development of renal end points in type 2 diabetes mellitus: systematic review and meta-analysis intensive glucose control in type 2 diabetes. Arch Intern Med. 2012;172(10):761–9.
8. Fu H, Liu S, Bastacky SI, Wang X, Tian XJ, Zhou D. Diabetic kidney diseases revisited: a new perspective for a new era. Mol Metab. 2019;30:250–63.
9. Govindaraj J, Sorimuthu Pillai S. Rosmarinic acid modulates the antioxidant status and protects pancreatic tissues from glucolipotoxicity mediated oxidative stress in high-fat diet: streptozotocin-induced diabetic rats. Mol Cell Biochem. 2015;404(1–2):143–59.
10. Hansen JB, Dos Santos LRB, Liu Y, Prentice KJ, Teudt F, Tonnesen M, Jonas JC, Wheeler MB, Mandrup-Poulsen T. Glucolipotoxic conditions induce β-cell iron import, cytosolic ROS formation and apoptosis. J Mol Endocrinol. 2018;61(2):69–77.
11. Kowluru A, Kowluru RA. Phagocyte-like NADPH oxidase [Nox2] in cellular dysfunction in models of glucolipotoxicity and diabetes. Biochem Pharmacol. 2014;88(3):275–83.
12. Xie SY, Liu SQ, Zhang T, Shi WK, Xing Y, Fang WX, Zhang M, Chen MY, Xu SC, Fan MQ, et al. USP28 serves as a key suppressor of mitochondrial morpho-functional defects and cardiac dysfunction in the diabetic heart. Circulation. 2024;149(9):684–706.
13. Huang Q, You W, Li Y, Sun Y, Zhou Y, Zhang Y, Liu D, Zhan S, Zhu Y, Han X. Glucolipotoxicity-inhibited miR-299-5p regulates pancreatic β-Cell function and survival. Diabetes. 2018;67(11):2280–92.
14. Palomer X, Salvadó L, Barroso E, Vázquez-Carrera M. An overview of the crosstalk between inflammatory processes and metabolic dysregulation during diabetic cardiomyopathy. Int J Cardiol. 2013;168(4):3160–72.
15. Wang L, Cai Y, Jian L, Cheung CW, Zhang L, Xia Z. Impact of peroxisome proliferator-activated receptor-α on diabetic cardiomyopathy. Cardiovasc Diabetol. 2021;20(1):2.
16. Cai L, Kang YJ. Oxidative stress and diabetic cardiomyopathy: a brief review. Cardiovasc Toxicol. 2001;1(3):181–93.
17. Wilson AJ, Gill EK, Abudalo RA, Edgar KS, Watson CJ, Grieve DJ. Reactive oxygen species signalling in the diabetic heart: emerging prospect for therapeutic targeting. Heart. 2018;104(4):293–9.
18. Cai L, Kang YJ. Cell death and diabetic cardiomyopathy. Cardiovasc Toxicol. 2003;3(3):219–28.
19. Bi Y, Liu S, Qin X, Abudureyimu M, Wang L, Zou R, Ajoolabady A, Zhang W, Peng H, Ren J, et al. FUNDC1 interacts with GPx4 to govern hepatic ferroptosis and fibrotic injury through a mitophagy-dependent manner. J Adv Res. 2024;55:45–60.
20. Niu B, Liao K, Zhou Y, Wen T, Quan G, Pan X, Wu C. Application of glutathione depletion in cancer therapy: enhanced ROS-based therapy, ferroptosis, and chemotherapy. Biomaterials. 2021;277: 121110.
21. Dixon SJ, Lemberg KM, Lamprecht MR, Skouta R, Zaitsev EM, Gleason CE, Patel DN, Bauer AJ, Cantley AM, Yang WS, et al. Ferroptosis: an iron-dependent form of nonapoptotic cell death. Cell. 2012;149(5):1060–72.
22. Stockwell BR, Friedmann Angeli JP, Bayir H, Bush AI, Conrad M, Dixon SJ, Fulda S, Gascón S, Hatzios SK, Kagan VE, et al. Ferroptosis: a regulated cell death nexus linking metabolism, redox biology, and disease. Cell. 2017;171(2):273–85.
23. Fang X, Wang H, Han D, Xie E, Yang X, Wei J, Gu S, Gao F, Zhu N, Yin X, et al. Ferroptosis as a target for protection against cardiomyopathy. Proc Natl Acad Sci U S A. 2019;116(7):2672–80.
24. Fang X, Cai Z, Wang H, Han D, Cheng Q, Zhang P, Gao F, Yu Y, Song Z, Wu Q, et al. Loss of cardiac ferritin H facilitates cardiomyopathy via Slc7a11-mediated ferroptosis. Circ Res. 2020;127(4):486–501.
25. Swaminathan S, Fonseca VA, Alam MG, Shah SV. The role of iron in diabetes and its complications. Diabetes Care. 2007;30(7):1926–33.
26. Liu Q, Sun L, Tan Y, Wang G, Lin X, Cai L. Role of iron deficiency and overload in the pathogenesis of diabetes and diabetic complications. Curr Med Chem. 2009;16(1):113–29.
27. White DL, Collinson A. Red meat, dietary heme iron, and risk of type 2 diabetes: the involvement of advanced lipoxidation endproducts. Adv Nutr. 2013;4(4):403–11.
28. Doll S, Freitas FP, Shah R, Aldrovandi M, da Silva MC, Ingold I, Goya Grocin A, Xavier da Silva TN, Panzilius E, Scheel CH, et al. FSP1 is a glutathione-independent ferroptosis suppressor. Nature. 2019;575(7784):693–8.
29. Shu Z, Chen S, Xiang H, Wu R, Wang X, Ouyang J, Zhang J, Liu H, Chen AF, Lu H. AKT/PACS2 participates in renal vascular hyperpermeability by regulating endothelial fatty acid oxidation in diabetic mice. Front Pharmacol. 2022;13: 876937.
30. Simmen T, Aslan JE, Blagoveshchenskaya AD, Thomas L, Wan L, Xiang Y, Feliciangeli SF, Hung CH, Crump CM, Thomas G. PACS-2 controls endoplasmic reticulum-mitochondria communication and Bid-mediated apoptosis. Embo j. 2005;24(4):717–29.
31. Arruda AP, Pers BM, Parlakgül G, Güney E, Inouye K, Hotamisligil GS. Chronic enrichment of hepatic endoplasmic reticulum-mitochondria contact leads to mitochondrial dysfunction in obesity. Nat Med. 2014;20(12):1427–35.
32. Houten SM, Violante S, Ventura FV, Wanders RJ. The biochemistry and physiology of mitochondrial fatty acid β-oxidation and its genetic disorders. Annu Rev Physiol. 2016;78:23–44.
33. Liang K. Mitochondrial CPT1A: insights into structure, function, and basis for drug development. Front Pharmacol. 2023;14:1160440.
34. Bonnefont JP, Djouadi F, Prip-Buus C, Gobin S, Munnich A, Bastin J. Carnitine palmitoyltransferases 1 and 2: biochemical, molecular and medical aspects. Mol Aspects Med. 2004;25(5–6):495–520.
35. Holubarsch CJ, Rohrbach M, Karrasch M, Boehm E, Polonski L, Ponikowski P, Rhein S. A double-blind randomized multicentre clinical trial to evaluate the efficacy and safety of two doses of etomoxir in comparison with placebo in patients with moderate congestive heart failure: the ERGO (etomoxir for the recovery of glucose oxidation) study. Clin Sci (Lond). 2007;113(4):205–12.
36. Deprince A, Haas JT, Staels B. Dysregulated lipid metabolism links NAFLD to cardiovascular disease. Mol Metab. 2020;42: 101092.
37. Weber M, Mera P, Casas J, Salvador J, Rodríguez A, Alonso S, Sebastián D, Soler-Vázquez MC, Montironi C, Recalde S, et al. Liver CPT1A gene therapy reduces diet-induced hepatic steatosis in mice and highlights potential lipid biomarkers for human NAFLD. Faseb j. 2020;34(9):11816–37.
38. Mao C, Liu X, Zhang Y, Lei G, Yan Y, Lee H, Koppula P, Wu S, Zhuang L, Fang B, et al. DHODH-mediated ferroptosis defence is a targetable vulnerability in cancer. Nature. 2021;593(7860):586–90.
39. Wang M, Song L, Strange C, Dong X, Wang H. Therapeutic effects of adipose stem cells from diabetic mice for the treatment of type 2 diabetes. Mol Ther. 2018;26(8):1921–30.
40. Cheng Y, Yu X, Zhang J, Chang Y, Xue M, Li X, Lu Y, Li T, Meng Z, Su L, et al. Pancreatic kallikrein protects against diabetic retinopathy in KK Cg-A(y)/J and high-fat diet/streptozotocin-induced mouse models of type 2 diabetes. Diabetologia. 2019;62(6):1074–86.
41. Sun J, Huang X, Niu C, Wang X, Li W, Liu M, Wang Y, Huang S, Chen X, Li X, et al. aFGF alleviates diabetic endothelial dysfunction by decreasing oxidative stress via Wnt/β-catenin-mediated upregulation of HXK2. Redox Biol. 2021;39: 101811.
42. Wu L, Liu C, Chang DY, Zhan R, Zhao M, Man Lam S, Shui G, Zhao MH, Zheng L, Chen M. The attenuation of diabetic nephropathy by Annexin A1 via regulation of lipid metabolism through the AMPK/PPARα/CPT1b pathway. Diabetes. 2021;70(10):2192–203.
43. Liu Y, Wan Y, Jiang Y, Zhang L, Cheng W. GPX4: the hub of lipid oxidation, ferroptosis, disease and treatment. Biochim Biophys Acta Rev Cancer. 2023;1878(3): 188890.
44. Tian Y, Xie Y, Guo Z, Feng P, You Y, Yu Q. 17β-oestradiol inhibits ferroptosis in the hippocampus by upregulating DHODH and further improves memory decline after ovariectomy. Redox Biol. 2023;62: 102708.
45. Gao M, Yi J, Zhu J, Minikes AM, Monian P, Thompson CB, Jiang X. Role of mitochondria in ferroptosis. Mol Cell. 2019;73(2):354–63.
46. Zorzano A, Liesa M, Palacín M. Mitochondrial dynamics as a bridge between mitochondrial dysfunction and insulin resistance. Arch Physiol Biochem. 2009;115(1):1–12.
47. Diaz-Morales N, Rovira-Llopis S, Bañuls C, Escribano-Lopez I, de Marañon AM, Lopez-Domenech S, Orden S, Roldan-Torres I, Alvarez A, Veses S, et al. Are

mitochondrial fusion and fission impaired in leukocytes of type 2 diabetic patients? Antioxid Redox Signal. 2016;25(2):108–15.
48. Thomas G, Aslan JE, Thomas L, Shinde P, Shinde U, Simmen T. Caught in the act-protein adaptation and the expanding roles of the PACS proteins in tissue homeostasis and disease. J Cell Sci. 2017;130(11):1865–76.
49. Wieckowski MR, Giorgi C, Lebiedzinska M, Duszynski J, Pinton P. Isolation of mitochondria-associated membranes and mitochondria from animal tissues and cells. Nat Protoc. 2009;4(11):1582–90.
50. Malone JI, Hansen BC. Does obesity cause type 2 diabetes mellitus (T2DM)? Or is it the opposite? Pediatr Diabetes. 2019;20(1):5–9.
51. Wu QR, Zheng DL, Liu PM, Yang H, Li LA, Kuang SJ, Lai YY, Rao F, Xue YM, Lin JJ, et al. High glucose induces Drp1-mediated mitochondrial fission via the Orai1 calcium channel to participate in diabetic cardiomyocyte hypertrophy. Cell Death Dis. 2021;12(2):216.
52. Wang X, Chen X, Zhou W, Men H, Bao T, Sun Y, Wang Q, Tan Y, Keller BB, Tong Q, et al. Ferroptosis is essential for diabetic cardiomyopathy and is prevented by sulforaphane via AMPK/NRF2 pathways. Acta Pharm Sin B. 2022;12(2):708–22.
53. Rovira-Llopis S, Bañuls C, Diaz-Morales N, Hernandez-Mijares A, Rocha M, Victor VM. Mitochondrial dynamics in type 2 diabetes: pathophysiological implications. Redox Biol. 2017;11:637–45.

Publisher's Note